Chapter 1.

Andrzej CHMIELOWIEC[1*]
Wojciech HOMIK[2]

MODELLING OF A TORSIONAL VIBRATIONS VISCOUS DAMPER USING THE HYDRODYNAMIC THEORY OF ROTATING ELEMENTS LUBRICATION

Abstract
Viscous dampers are one of the ways of reducing torsional vibrations in multi-cylinder internal combustion engine crankshafts. The damping element often used in this type of devices is a plunger immersed in silicone oil of very high viscosity. Until now the state of a damper has been modelled based on rather idealized assumptions and without any hydrodynamic analysis of the state of oil inside it. Unfortunately such models do not explain the reasons behind excessive and too fast wear of oil and the active surfaces of the damper. Searching for the causes of damper breakdowns, the authors decided to develop a new mathematical model based on the rotating elements lubrication theory. This paper explains the hydrodynamic modelling of a torsional vibrations viscous damper and discusses the problems that must be solved so that the model can be developed.

Keywords:
tribology, hydrodynamic modelling, lubrication theory, torsional vibrations, vibrations damping, viscous damper

1. Introduction
The second part of this paper outlines the issue of torsional vibrations occurring in combustion engines. Apart from a general characteristic of this problem, it also provides an insight into the methods used so far to model torsional vibration

[1] Faculty of Mechanics and Technology, Rzeszow University of Technology, al. Powstańców Warszawy 12, 35-959 Rzeszów, Poland
[2] Faculty of Mechanical Engineering and Aeronautics, Rzeszow University of Technology, al. Powstańców Warszawy 12, 35-959 Rzeszów, Poland
[*]e-mail: achmie@prz.edu.pl

dampers. The third part proposes to add hydrodynamic modelling of the effects that occur during the operation of the said dampers to the methods used so far. The initial numerical results allow us to suspect that this type of modelling may substantially contribute to this field of science.

2. Torsional vibrations in multi-cylinder combustion engines

The main source of vibrations in a multi-cylinder combustion engine is the performance of the crank and piston system, or strictly speaking, the conversion of reciprocating motion into circular motion. A kinematic analysis of a crank system may be conducted if we replace a real system with the diagram presented in Figure 1.1. The main geometric parameters characterising this diagram include [1, 2, 3, 5, 8, 9, 13, 14]:

1. length of connecting rod $l = AB$ (measured from the axis of the piston pin to the axis of the crankpin),
2. crank throw $r = BO = S / 2$,
3. piston stroke S (measured as the distance travelled by the piston between TDC and BDC),

ratio of crank throw r to the crank length $\lambda = r / l$.

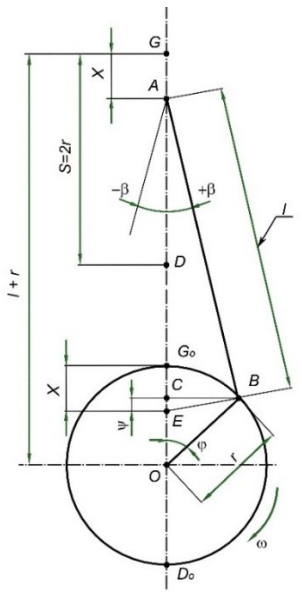

Fig. 1.1. Diagram of a simple crank system

In a real crank system the motion of the piston is not exactly harmonic. Piston velocity c in function of the angle of rotation of the shaft φ is given by [2, 3]:

$$c(\varphi) = \frac{dx}{dt} = r\omega\left(\sin\varphi + \frac{\lambda}{2}\sin 2\varphi\right) = r\omega\sin\varphi + r\omega\frac{\lambda}{2}\sin 2\varphi. \quad (1)$$

Figure 1.2 shows a graph of piston velocity *c* and its two harmonic components.

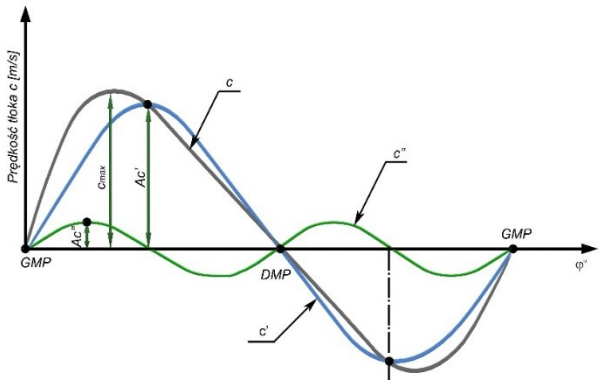

Fig. 1.2. Piston velocity $c = c' + c''$ in function of the angle of rotation of the crankshaft φ

By differentiating equation (1) with respect to time, we obtain the relation of piston acceleration *b* in function of the angle of rotation of crankshaft φ:

$$b(\varphi) = \frac{dc}{dt} = r\omega^2\cos\varphi + r\omega^2\lambda\cos 2\varphi. \quad (2)$$

Changes in constituent and resultant accelerations in function of the angle of rotation of the shaft are analysed in Figure 1.3.

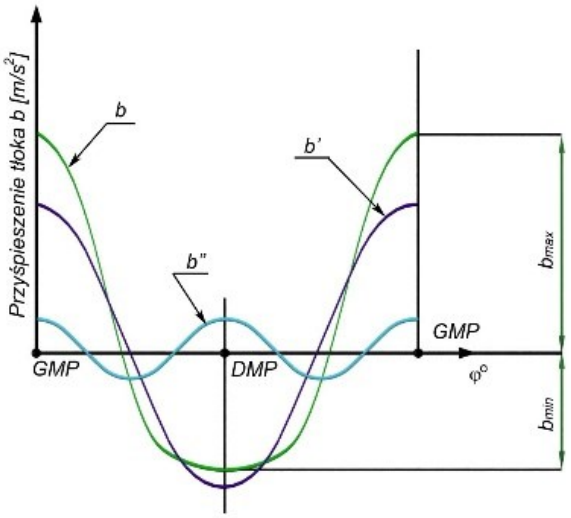

Fig. 1.3. Changes in piston acceleration $b = b' + b''$ in function of angle φ

The source of the above accelerations are forces which act upon the crank system and cause the crankshaft of the engine to vibrate. These forces include (Figure 1.4) [2, 3, 5, 13, 14]:

1. gas pressure forces generated in the mixture combustion process,
2. inertia forces originating from the masses in reciprocating and circular motion (sliding forces and centrifugal forces).

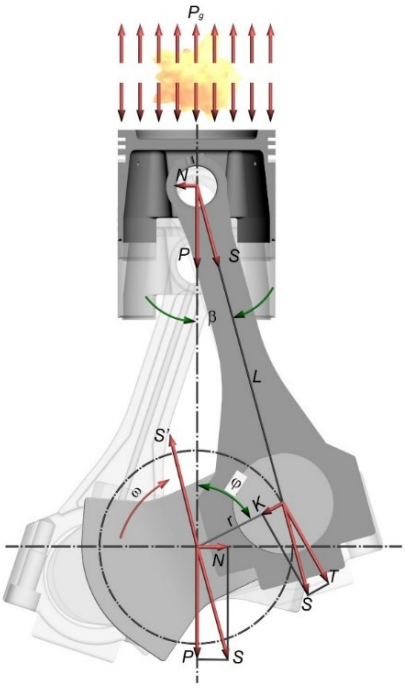

Fig. 1.4. Balance of forces in a crank and piston system

Gas pressure forces P_g and inertia forces P_b change periodically [2, 3, 1, 14]. In four-stroke engines the inertia forces change during one full turn of the crankshaft, while gas pressure forces change during two turns of the crankshaft or one full turn in two-stroke engines. The resultant force is the sum of the forces mentioned above:

$$P = P_g + P_b. \tag{3}$$

As shown in Figure 1.4, force S acts upon the crank of the crankshaft and decomposes into two components: component T tangent to the circle drawn by the crank throw and radial component K operating along the temporary location of the crank arm. The forces are characterised by the following relations:

$$T = S\,sin(\alpha + \beta) = \frac{P}{cos\,\beta} sin(\alpha + \beta), \tag{4}$$

$$K = S\,cos(\alpha + \beta) = \frac{P}{cos\,\beta} cos(\alpha + \beta). \tag{5}$$

Periodic changes in gas pressure forces P_g and inertia forces P_p generate the following types of crankshaft vibrations [2, 3, 1, 5, 14]:

1. transverse vibrations,
2. longitudinal vibrations,
3. torsional vibrations.

Vibrations are a kind of defence available to machine parts made of elastic materials, which makes them give in to the imposed load and gradually absorb the energy transferred to them.

Regardless of the dynamic system in which the engine operates, the greatest threat to the crankshaft is posed by torsional vibrations [2, 3, 1, 5, 13, 14]. The source of torsional vibrations is the periodic variability of force *T*. It is worth stressing that the scale of torsional vibrations is limited only by the torsional stiffness of the shaft and when the vibrations are not damped, their amplitude theoretically tends to infinity. Once the maximum amplitude is exceeded, the shaft breaks down.

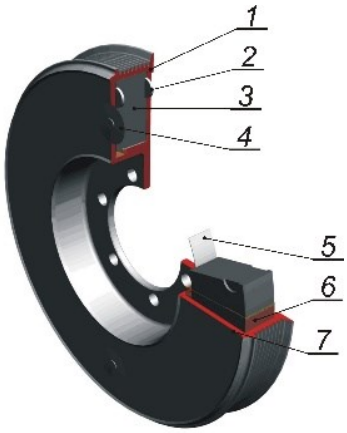

Fig. 1.5. Viscous torsional vibration damper: 1 - housing of the damper, 2 - thrust bearing, 3 - inertia ring, 4 - seal, 5 - radial bearing, 6 - silicone oil, 7 - cover

In order to minimize the threat posed by torsional vibrations, devices called torsional vibration dampers are used. Most frequently they are located at the free end of the crankshaft of the engine [2, 3]. Over the years, the following types of dampers have been used [2, 3]:

1. friction dampers,
2. viscous dampers,
3. rubber dampers,
4. spring dampers.

Viscous torsional vibration dampers are most frequently used in medium and large-size multi-cylinder combustion engines (Figure 1.5).

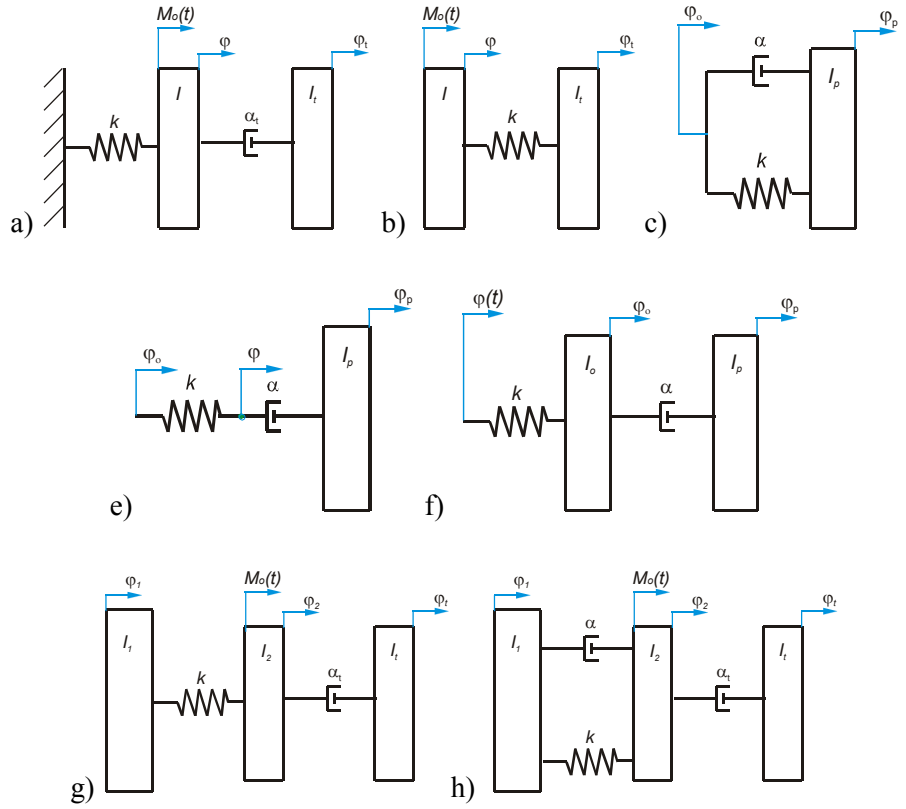

Fig. 1.6. Examples of damper modelling: a) viscous damper with torque $M(t)$ applied to the housing, b) dynamic damper with torque $M(t)$ applied to the hub, c) rubber damper with kinematic torque applied to the hub, d) viscous damper with viscoelastic fluid (Maxwell's model) with kinematic torque, e) dual mass model of a viscous damper with kinematic torque, f) model of a system comprising a viscous damper with reduced moment of inertia of the crank and piston system and torque $M(t)$ applied to the hub, g) model of a system comprising a viscous damper with reduced moment of inertia of the crank and piston system with damped inner shaft and torque $M(t)$ applied to the hub.

Viscous torsional vibration dampers are designed individually for every type of engines (power transmission systems) based on the results of a harmonic analysis of torsional vibrations in the shaft (e.g. the crankshaft or the camshaft). Before the work on designing a new damper starts, the engine producer should provide

the designer with an appropriate set of data about the engine, including data on the basic units supporting the engine [2, 3]. Based on these data, a model of the power transmission system comprising a model of the damper is built. In practice, a variety of methods are used to model torsional vibration dampers [2, 3]. Discrete systems provide an adequate approximation.

Most frequently viscous dampers are modelled as dual mass systems (Figure 1.7). The masses are interconnected by damping element α_w. Periodic torque $M(t)$ is applied to mass I_w connected with spring element k_w. The other end of the spring is immobilized, which corresponds to the node of the first form of torsional vibrations [2, 3].

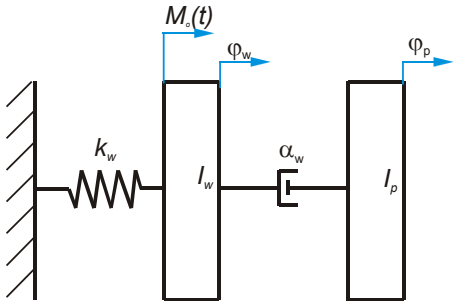

Figure 1.7. Discrete model of a viscous torsional vibration damper

Damping function α_w in a viscous torsional vibration damper depends on many variables, including in particular:

1. kinetic viscosity of the fluid,
2. dynamic viscosity of the fluid,
3. density of the fluid,
4. size of clearances,
5. mass moment of inertia of the inertia ring of the damper.

They affect the value of the damper's moment of friction, which in turn directly translates into the volume of energy dispersed by the damper [10, 15].

Analytical calculations for viscous dampers are made mainly based on models assuming linear spring element and linear damping. While the first assumption is roughly met, the second one about fluid being linear may prove to be an oversimplification, especially in the case of fluids of viscosity greater than 500,000 [cSt]. Therefore, it seems advisable to enrich the modelling of viscous torsional vibration dampers with elements of hydrodynamic modelling.

3. Elements of hydrodynamic modelling of the viscous torsional vibration damper

The discrete model presented in the previous section is quite accurate in predicting the performance of a damper in the steady state. However, it provides no information on how a damper performs in the start-up phase and when it is displaced from the steady state, e.g. by an abrupt external acceleration. The modelling of such conditions may prove particularly vital due to the fact that we are currently unable to answer the questions about mechanical damage occurring to a damper during its operation. Periodic inspections revealed dampers with seriously damaged active surfaces of the housing and the plunger, and with oil having a gel-like or even solid consistency. Since no one has yet proposed an explanation for such situations, we felt inclined to develop a model capable of at least partly explaining the reasons behind them. Therefore, in the next sections we will present certain elements of a theory of hydrodynamic modelling of the performance of a viscous torsional vibration damper.

However, before we get to that, we must define the terms and symbols that will be used later on to describe the geometry of a viscous damper. Figure 1.8 shows active surfaces of a plunger (an inertia ring in this particular case). Among others, a plunger consists of:

1. outer surface of the plunger - Figure 1.8 a),
2. lateral surface of the plunger - Figure 1.8 b),
3. inner surface of the plunger - Figure 1.8 c).

For each surface of the plunger there is a matching surface of the housing named analogically, i.e. outer surface of the housing, lateral surface of the housing and inner surface of the housing.

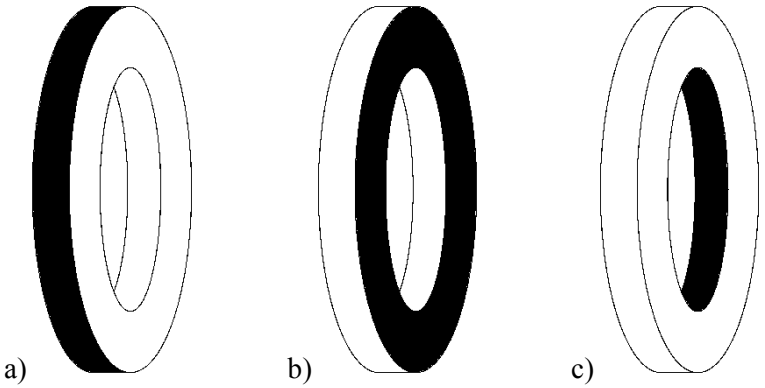

Figure 1.8. Surfaces of the plunger: a) outer surface, b) lateral surface, c) inner surface

Figure 1.9 shows the radiuses of the outer and inner surfaces of both a plunger and the housing. We make an assumption that the inner radiuses may equal 0. If that is the case, the plunger has the shape of a cylinder.

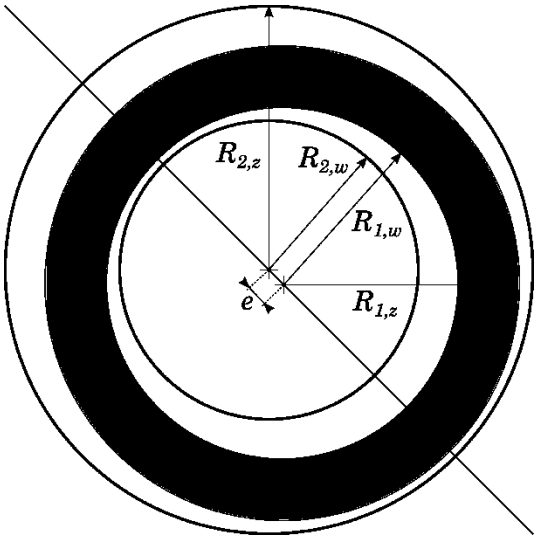

Fig. 1.9. Radiuses of the plunger and the housing: $R_{1,z}$ - outer radius of the plunger, $R_{1,w}$ - inner radius of the plunger, $R_{2,z}$ - outer radius of the housing, $R_{2,w}$ - inner radius of the housing, e - eccentricity

3.1. Basics of the rotating elements wet friction theory

At the end of the 19th century, Reynolds [11] proposed an equation for determining the pressure of a fluid film residing between two hard, moving surfaces. It turns out that if:

1. the fluid flow is laminar,
2. the force of gravity and the force of inertia are negligibly small compared to the force of viscosity,
3. the fluid is incompressible,
4. the fluid is Newtonian with constant viscosity,
5. the pressure of the fluid remains unchanged across the film's height,
6. the rate of change of velocity in directions x and z is negligibly small compared to the rate of change of velocity in direction y,
7. there is no slipping between the fluid and the surface touching it,

the fluid pressure equation takes the following form:

$$\frac{\partial}{\partial x}\left(h^3\frac{\partial p}{\partial x}\right)+\frac{\partial}{\partial z}\left(h^3\frac{\partial p}{\partial z}\right)=6\eta\left[(U_1+U_2)\frac{\partial h}{\partial x}+2V_2\right], \tag{6}$$

where η is fluid viscosity, p is pressure and the remaining values are defined in Figure 1.10.

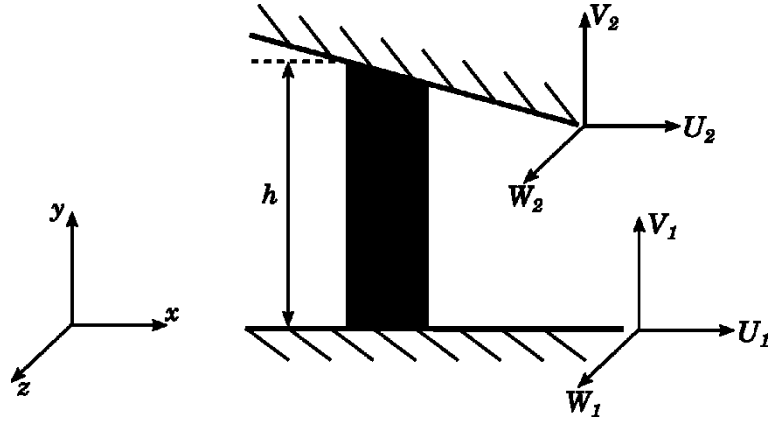

Fig. 1.10. Absolute velocities of the surfaces between which the analysed fluid resides

It must be stressed that in the form presented above the equation assumes that axis x was chosen as the direction of the relative motion of both surfaces. Consequently, we can assume that $V_1 = W_1 = W_2 = 0$. If we additionally assume that there is no flow towards axis z, the Reynolds equation is simplified to:

$$\frac{\partial}{\partial x}\left(h^3 \frac{\partial p}{\partial x}\right) = 6\eta U_1 \frac{\partial h}{\partial x}. \tag{7}$$

Using the Reynolds equation we can determine the pressure of the oil film residing between the outer and inner surfaces of the plunger and the housing. For this purpose we use a model assuming that oil does not flow in the axial direction (z) of both of these elements. In addition, we assume that ϕ from range [0, 2π] is the angular coordinate for which pressure is calculated, η is oil viscosity, R_z and R_w are outer and inner radiuses of the plunger and the housing (we assume that for the purpose of the Reynolds theory $R_z = R_{1,z} = R_{2,z}$ and $R_w = R_{1,w} = R_{2,w}$), u_z and u_w are relative velocities of the plunger and the housing respectively in the outer and inner layer, which satisfy the relation $u_z = u_w R_z/R_w$,, $c_z = R_{2,z} - R_{1,z}$ is outer radial clearance, $c_w = R_{1,w} - R_{2,w}$ is inner radial clearance, $\varepsilon_z = e/c_z$ is outer relative eccentricity, and $\varepsilon_w = e/c_w$ is inner relative eccentricity. At this point, it is worth stressing that in practice the outer radial clearance of a damper is greater than the inner radial clearance. Consequently, the plunger may touch the housing only on the inner surface on which the bearing tape is also placed. In practice, this means that the relative inner eccentricity ε_w may take values from range [0, 1]

and the relative outer eccentricity ε_z is restricted to range [0, δ], where $\delta < 1$. Using the above symbols, we can express the oil film pressure in the outer and inner slot by the following formula [4]:

$$p_\phi = \frac{6\eta u R}{c^2}\left[\int \frac{d\phi}{(1+\varepsilon\cos\phi)^2} - \frac{h_m}{c}\int \frac{d\phi}{(1+\varepsilon\cos\phi)^3}\right] + C_2, \tag{8}$$

where R is radius of curvature of the slot, u is relative velocity of the surfaces of the slot, c is radial clearance of the slot, h_m is height of the oil film where the pressure is the highest and C_2 is the integration constant.
In order to solve the following integrals:

$$\int \frac{d\phi}{(1+\varepsilon\cos\phi)^n} \tag{9}$$

we use the substitution proposed by Sommerfeld [4, 12]:

$$1 + \varepsilon\cos\phi = \frac{1-\varepsilon^2}{1-\varepsilon\cos\varphi} \tag{10}$$

where φ is a new variable with range of variation [0, 2π] – the same as for variable ϕ. In addition, the change of variables results in the following transformations $0 \to 0$, $\pi \to \pi$ and $2\pi \to 2\pi$. For a substitution expressed this way the following relations are true:

$$J_1 = \int \frac{d\phi}{(1+\varepsilon\cos\phi)} = K\varphi, \tag{11}$$

$$J_2 = \int \frac{d\phi}{(1+\varepsilon\cos\phi)^2} = K^3(\varphi - \varepsilon\sin\varphi), \tag{12}$$

$$J_3 = \int \frac{d\phi}{(1+\varepsilon\cos\phi)^3} = K^5\left(\varphi - 2\varepsilon\sin\varphi + \frac{\varepsilon^2}{2}\varphi + \frac{\varepsilon^2}{4}\sin 2\varphi\right), \tag{13}$$

where $K = 1/\sqrt{1-\varepsilon^2}$.
Using these symbols, the oil film pressure in function of angle may be expressed as follows:

$$p_\phi = \frac{6\eta u R}{c^2}\left[J_2(\varphi) - \frac{h_m}{c}J_3(\varphi)\right] + C_2, \tag{14}$$

For the completeness of the above formula it is necessary to determine integration constants h_m and C_2. We can achieve this by assuming specific pressure values. In this particular case we assume that [6]: $p_\phi(0) = p_\varphi(0) = p_0$ and $p_\phi(2\pi) = p_\varphi(2\pi) =$

p_0, while the equality of pressures $p_\phi(0) = p_\varphi(0)$ and $p_\phi(2\pi) = p_\varphi(2\pi)$ results from the fact that the applied substitution $\phi \rightarrow \varphi$ transforms $0 \rightarrow 0$ and $2\pi \rightarrow 2\pi$. Determining a specific value of p_0 is not obvious, as it depends, among others, from the absolute angular velocity of both the housing and the plunger. We will analyse this problem in greater detail further in this paper. Ultimately, for constants:

$$h_m = \frac{2(1-\varepsilon^2)}{2+\varepsilon^2} c, \tag{15}$$

$$C_2 = p_0 \tag{16}$$

and after returning to the original variable ϕ, we obtain:

$$p(\phi) = p_0 + \frac{6\eta u R}{c^2} \frac{\varepsilon(2+\varepsilon\cos\phi)\sin\phi}{(2+\varepsilon^2)(1+\varepsilon\cos\phi)^2} = p_0 + \frac{6\eta u R}{c^2}\gamma(\varepsilon,\phi), \tag{17}$$

where γ is a dimensionless distribution of the oil film pressure, whose graph for several ε values is shown in Figure 1.11.

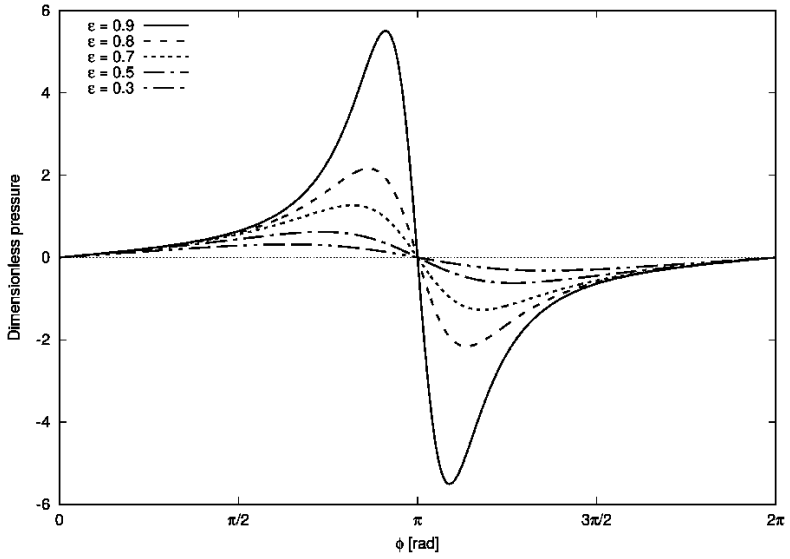

Fig. 1.11. Graph of dimensionless pressure γ for several ε values

3.2. Gümbel's condition for the inertia ring

Gümbel's condition was originally proposed for improved modelling of the oil film forces in high pressure conditions. Gümbel postulated that $p_0 = 0$ and that the negative part of pressure $p(\phi)$ equals zero. What it means is that the pressure function is exactly the same as that proposed by Sommerfeld for range $[0, \pi]$, while for range $[\pi, 2\pi]$ it equals zero. Figure 1.12 shows the parts of the oil film generating actual force under Gümbel's assumptions.

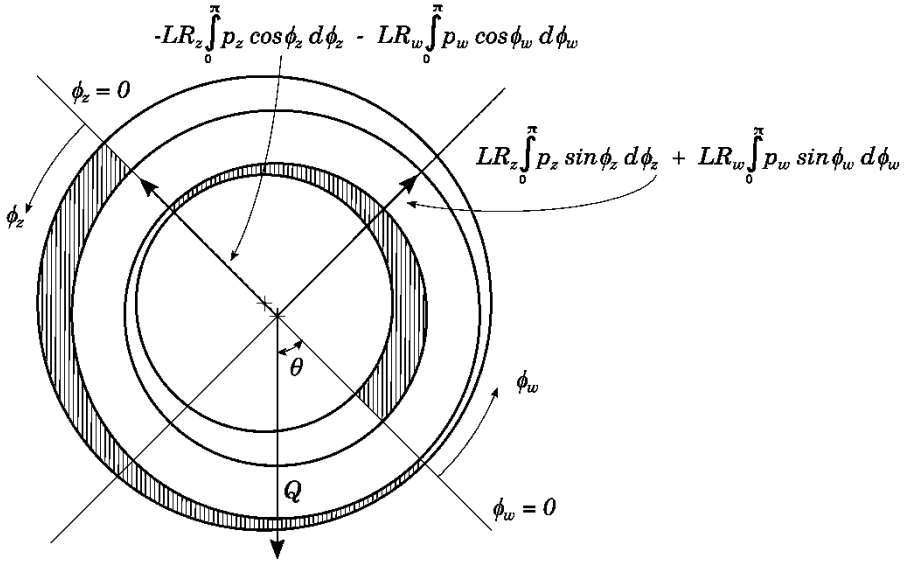

Fig. 1.12. Balance of forces for Gümbel's condition in the case of a ring-shaped plunger

An analysis of forces in the presented system leads to an equilibrium condition in which the oil film pressure entirely counterbalances the weight of the inertia ring Q.

$$Q\cos\theta = -LR_z\int_0^{\pi} p_z \cos\phi_z d\phi_z - LR_w\int_0^{\pi} p_w \cos\phi_w d\phi_w, \tag{18}$$

$$Q\sin\theta = LR_z\int_0^{\pi} p_z \sin\phi_z\, d\phi_z + LR_w\int_0^{\pi} p_w \sin\phi_w\, d\phi_w, \tag{19}$$

where L is the width of the inertia ring. In order to determine equilibrium angle θ, first we need to solve the following integrals:

$$\int_0^{\pi} p \sin\phi \, d\phi, \tag{20}$$

$$\int_0^{\pi} p \cos\phi \, d\phi. \tag{21}$$

We use integration by parts to solve both integrals:

$$\int_0^{\pi} p \sin\phi \, d\phi = [-p \cos\phi]_0^{\pi} + \int_0^{\pi} \frac{dp}{d\phi} \cos\phi \, d\phi = \int_0^{\pi} \frac{dp}{d\phi} \cos\phi \, d\phi, \tag{22}$$

$$\int_0^{\pi} p \cos\phi \, d\phi = [p \sin\phi]_0^{\pi} - \int_0^{\pi} \frac{dp}{d\phi} \sin\phi \, d\phi = -\int_0^{\pi} \frac{dp}{d\phi} \sin\phi \, d\phi, \tag{23}$$

Taking into account equation (8), we obtain:

$$\frac{dp}{d\phi} = \frac{6\eta u R}{c^2} \left[\frac{1}{(1+\varepsilon \cos\phi)^2} - \frac{h_m}{c} \frac{1}{(1+\varepsilon \cos\phi)^3} \right], \tag{24}$$

which allows us to calculate integrals (22) and (23). After making calculations for outer and inner surfaces, we obtain the following:

$$Q \cos\phi = \eta u_z L \left(\frac{R_z}{c_z}\right)^2 \frac{12\varepsilon_z^2}{(2+\varepsilon_z^2)(1-\varepsilon_z^2)} + \eta u_w L \left(\frac{R_w}{c_w}\right)^2 \frac{12\varepsilon_w^2}{(2+\varepsilon_w^2)(1-\varepsilon_w^2)}, \tag{25}$$

$$Q \sin\phi = \eta u_z L \left(\frac{R_z}{c_z}\right)^2 \frac{6\pi\varepsilon_z}{(2+\varepsilon_z^2)(1-\varepsilon_z^2)} + \eta u_w L \left(\frac{R_w}{c_w}\right)^2 \frac{6\pi\varepsilon_w}{(2+\varepsilon_w^2)(1-\varepsilon_w^2)}. \tag{26}$$

Relations (25) and (26) allow us to determine the relationship between the relative velocity of the housing and the plunger, capacity of the oil film and the shape of the slot. They will form the basis for the numerical analysis conducted below.

3.3. Numerical analysis based on real data

We conducted a numerical analysis of an actual damper characterised by the following geometric parameters: $R_{1,w}$ = 74.685 [mm], $R_{1,z}$ = 109.480 [mm], $R_{2,w}$ = 74.605 [mm], $R_{2,z}$ = 109.705 [mm] and L = 28.500 [mm]. Both the housing and the inertia ring were made of steel of density 7800 [kg/m^3]. The fluid used was silicone oil of static viscosity 300000 [cSt] = 0.3 [m^2/s] and density 1000 [kg/m^3]. Using these data and equations (25) and (26) we determine the number of turns for a given ε_w that should be made by the housing against the inertia ring so that it remains in equilibrium. At this point, it must be stressed that the results show the relative number of turns, i.e. how many more turns are made by the housing per hour. Graphs in Figures 1.13 and 1.14 show how the number of relative turns changes depending on the relative inner eccentricity ε_w. Be reminded that the relative outer eccentricity ε_z satisfies the following equation:

$$\varepsilon_z = \varepsilon_w \frac{c_w}{c_z}, \tag{27}$$

which makes ε_w the only independent variable determining the number of relative turns of both components of the damper. In the light of experiments conducted in a company manufacturing viscous dampers, the graph shown in Figure 1.14 is particularly interesting. It shows that when inner relative eccentricity ε_w equals 0.005, the housing makes one additional turn per hour. Experimental research carried out in that period produced similar results. What it means is that models assuming that the housing and the ring are concentric in the steady state are entirely justified.

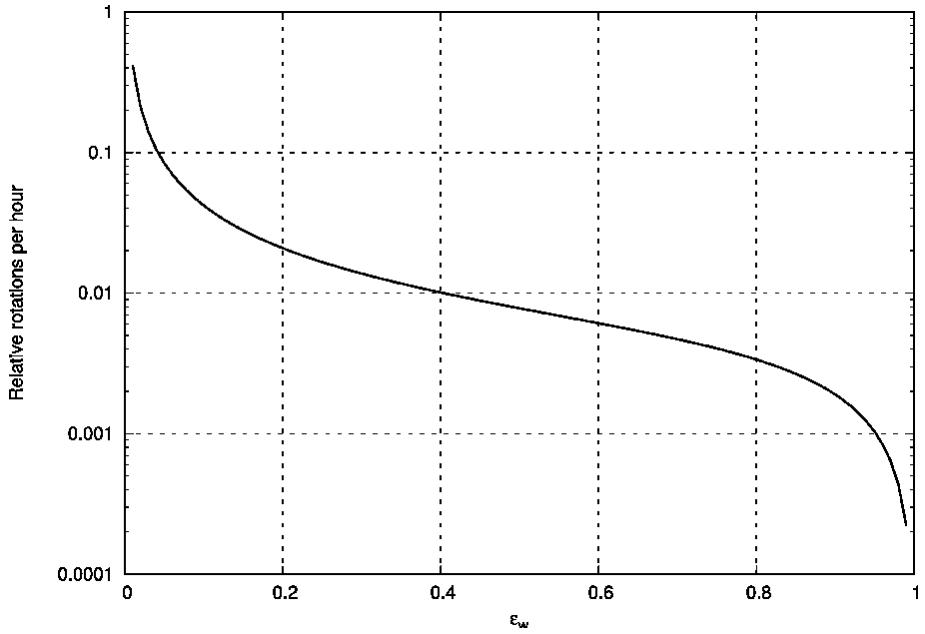

Figure 1.13. Number of turns of the housing against the inertia ring per hour, necessary for maintaining the ring in static equilibrium (range [0, 1])

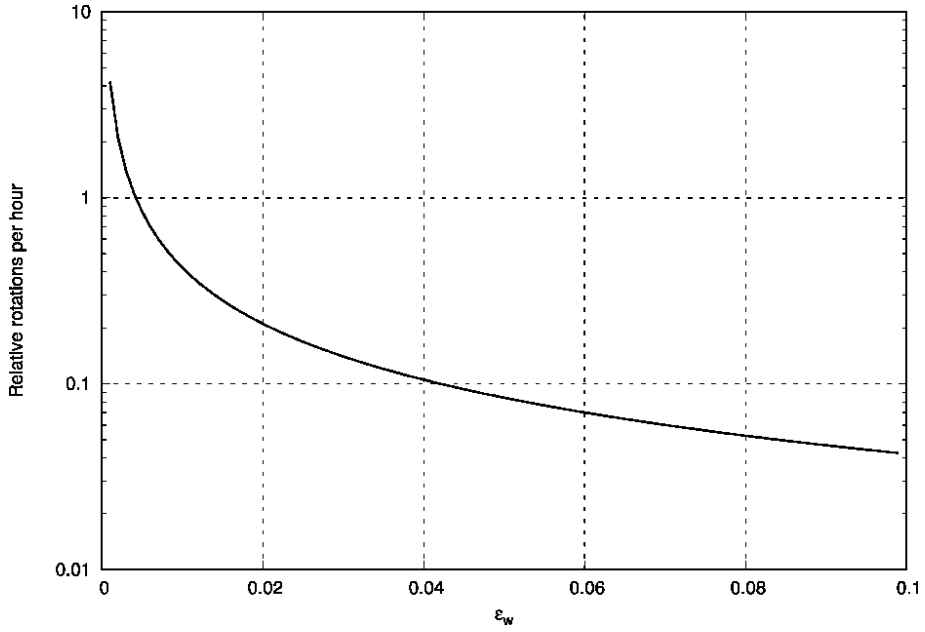

Figure 1.14. Number of turns of the housing against the inertia ring per hour, necessary for maintaining the ring in static equilibrium (range [0, 0.1])

4. Conclusions

This paper analyses the hydrodynamic effects occurring on the outer and inner surface of the inertia ring. The results of the numerical analysis conducted by the authors partially confirmed the results of experiments performed in a company manufacturing viscous dampers. Therefore, it seems legitimate to say that the presented approach is a step toward better understanding of the workings of a torsional vibration damper. However, the model outlined above does not comprehensively analyse this issue in its entirety. It must be clearly stated that the model does not cover the effects occurring on the lateral surfaces of the housing and the inertia ring, i.e. wet friction on these surfaces and increase in pressure p_0 caused by centrifugal force. The authors are continuing their research into this topic.

Research work carried out under contract No. U-18217 concluded between the DAMPOL Company implementing project no. POIR.01.01.01-00-0317/17 and the Rzeszów University of Technology. Project title: "Development of innovative technologies for the diagnosis and control of torsional vibration dampers in the crankshaft of an internal combustion engine and the selection of optimal methods for regeneration and repairs"

References

[1] Brun R. (1973). *Szybkobieżne silniki wysokoprężne*. WKiŁ.
[2] Homik W. (2012). *Szerokopasmowe tłumiki drgań skrętnych*. ITE-PIB. Radom.
[3] Homik W. (2015). *Wiskotyczne tłumiki drgań skrętnych*. ITE-PIB. Radom.
[4] Hori, Y. (2006). *Hydrodynamic Lubrication*. Springer-Verlag. Tokyo. DOI: 10.1007/4-431-27901-6
[5] Jędrzejowski J. (1986). *Mechanika układów korbowych silników samochodowych*. Wydawnictwa Komunikacji i Łacznosci, Warszawa.
[6] Langlois, W.E., Deville, M. (2014). *Slow Viscous Flow.* Springer International Publisching Switzerland. DOI: 10.1007/978-3-319-03835-3
[7] Maciotta R., Saija Merlino F. (1966). *Research on damping of torsional vibrations in the Dieselengined propelling plants.* FIAT Technical Bulletin 2.
[8] Niewiarowski K. (1986). *Tłokowe silniki spalinowe*. WKiŁ. Warszawa.
[9] Parszewski Z. (1976). *Teoria maszyn i mechanizmów*. WNT. Warszawa.
[10] Płowiec R. (1990). *Lepkość i sprężystość cieczy określana za pomocą ultradźwiękowych fal ścinania*. PWN. Warszawa - Poznań.
[11] Reynolds, O. (1886). On the Theory of Lubrication and its Application to Mr. B. Tower's Experiments. *Philosophical Transaction of Royal Society of London.* Vol. 177(1). pp. 157-234.
[12] Sommerfeld, A. (1904). Zur hydrodynamischen Theorie der Schmiermittelreibung. *Zeit. angew. Math. u. Physik.* Vol. 50. pp. 97-155.
[13] Wajand J.A. (1988). *Silniki o zapłonie samoczynnym*. WNT. Warszawa.
[14] Wajand J.A, Wajand J.T. (1993). *Tłokowe silniki spalinowe średnio i szybkoobrotowe*. WNT. Warszawa.
[15] Willkinson W. (1963). *L Ciecze nienewtonowskie*. WNT. Warszawa.